Reports

Elasticity of $MgSiO_3$ in the Perovskite Structure

A. YEGANEH-HAERI, D. J. WEIDNER, E. ITO

The single-crystal elastic moduli of $MgSiO_3$ in the perovskite structure, the high-pressure polymorph of $MgSiO_3$ pyroxene, have been determined. The data indicate that a mantle with either pyrolite or pyroxene stoichiometry is compatible with the seismic models appropriate to the earth's lower mantle, provided that the shear modulus of $MgSiO_3$ perovskite exhibits a strong negative temperature derivative. Such a temperature derivative falls outside of the range expected for a well-behaved refractory ceramic and could result if the pressure-temperature regime of the earth's lower mantle is near that required for a ferroelastic phase transformation of the perovskite phase.

THE MAJOR MINERALS OF THE earth's upper mantle undergo successive phase transitions to progressively higher density polymorphs and ultimately crystallize as a mixture of (Mg,Fe)O magnesiowustite and (Mg,Fe)SiO_3 in the perovskite structure under lower mantle conditions (*1*). Perovskite dominates the properties of the earth's lower mantle and constitutes as much as half of the volume of the earth. Some workers have suggested that the formation of perovskite is the cause of the 670-km seismic discontinuity. Tests of whether the mantle is chemically layered and of specific mineralogical models rely on comparisons of seismic observations with elastic properties of these high-pressure phases. We have determined the adiabatic single-crystal elastic moduli of $MgSiO_3$ perovskite under ambient conditions. In this report, we describe this measurement and discuss the significance of these results for the chemical composition of the lower mantle.

A large number of compounds with ABX_3 stoichiometry (A and B are cations; X represents the anion) crystallize in the perovskite structure (Fig. 1). This structure can be imagined as a network of regular BX_6 octahedra linked by their corners that extend symmetrically in three dimensions. The A cation occupies the cubical cavity formed by the eight octahedra and each is surrounded by 12 nearest neighbor anions (*2*). The ideal cubic structure occurs in only a few compounds. Because of variations in ionic size and small displacements of atoms, the most common structure for perovskite-type compounds is a pseudosymmetric variant of the ideal arrangement. This variant results from small distortions of the unit cell and reduction of the overall symmetry from cubic. Such distortions from the ideal arrangement commonly have large effects on the physical properties, and most likely produce the cooperative Jahn-Teller, ferroelectric, ferromagnetic, and ferroelastic properties of perovskites (*3*). At ambient conditions, the SiO_6 octahedra in $MgSiO_3$ perovskite are rotated and tilted to an orthorhombically distorted perovskite structure.

Nine elastic moduli are required for the complete definition of the elastic properties of $MgSiO_3$ perovskite (space group *Pbnm*). We determined each elastic modulus with Brillouin spectroscopy on single crystals (*4*) that were grown from a melt at a peak pressure of 27 GPa and temperature of 1830°C with a large volume, high-pressure uniaxial split-sphere apparatus (USSA-5000) (*5*). The crystals were 50 to 200 μm in diameter, optically transparent, colorless, and had (110)- and (001)-type growth faces. We examined each specimen for twinning with a four-circle x-ray diffractometer and precession x-ray photography and selected only twin-free transparent single crystals. The majority of the crystals were not twinned. We recorded a total of 65 spectra and averaged them into 34 compressional and shear acoustic velocities in 26 distinct crystallographic directions to define the velocity surface. These data were inverted to give the single-crystal elastic moduli (Table 1) and aggregate elastic properties (Table 2).

The large magnitudes of the single-crystal elastic moduli reflect the rigidity of the SiO_6 octahedron under compression and shear. In particular, the ratio of the shear modulus to bulk modulus for $MgSiO_3$ is larger than has been reported for any other compound in the perovskite structure. This behavior is consistent with earlier observations on the elastic properties of stishovite and $MgSiO_3$ ilmenite, where silicon is in sixfold coordination and which also exhibit a large shear modulus as compared with other oxides in the same crystal structures (*6*). Theoretical predictions of single-crystal elastic moduli with the potential induced breathing model (*7*) suggest that $MgSiO_3$ perovskite has a high shear modulus, consistent with our experimental data.

Earlier measurements of the bulk modulus for $MgSiO_3$ perovskite have been pressure-volume compression studies of samples with up to 11% iron replacing magnesium (*8–10*). Our measurement compares reasonably well with these values when the uncertainties of the compression studies are considered (Table 3).

A material is considered to be ferroelastic if it possesses two or more possible orientation states (twin domains) that are related by a macroscopic strain (*11*). For the twinned orthorhombic perovskite crystals that we grew, the twinning is consistent with an unit cell rotation of 90° about the c axis, such that the a axis in one set of domains lies parallel to the b axis in the other. Transformation from one twin state to the other, however, is accomplished by reversing the sense of one of the orthorhombic distortions with an effective shear strain of only a few degrees. This style of ferroelastic behavior is common in many distorted perovskite-type compounds, including the distorted rare-earth orthoaluminate- and orthoferrite-type perovskites, which are isostructural with $MgSiO_3$ perovskite (*12*). These materials generally exhibit ferroelastic-type phase transformations (either of first

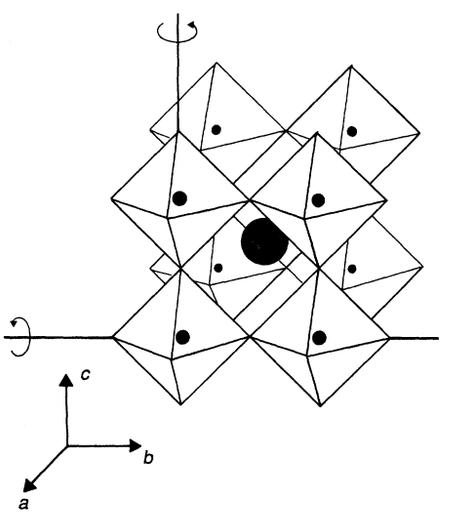

Fig. 1. Three-dimensional view of the ideal perovskite structure, illustrating chains of BX_6 octahedra. The rotations of these octahedra about their respective axis (as shown by the arrows) result in distortions of the unit cell and reduction of the overall symmetry from cubic.

A. Yeganeh-Haeri and D. J. Weidner, Department of Earth and Space Sciences, State University of New York, Stony Brook, NY 11794.
E. Ito, Institute for Study of the Earth's Interior, Okayama University, Misasa, Tottori-Ken 682-02, Japan.

Table 1. Single-crystal elastic moduli, C_{ij}, of $MgSiO_3$ perovskite. Errors (±1 SD) are in parentheses.

ij	C_{ij} (GPa)
11	515 (5)
22	525 (5)
33	435 (5)
44	179 (4)
55	202 (3)
66	175 (4)
12	117 (5)
13	117 (5)
23	139 (6)

Table 2. Aggregate elastic properties in gigapascals and acoustic velocities in kilometers per second for $MgSiO_3$ perovskite. The density is 4.108 g/cm^3, and the root-mean-square error is 0.11 km/s; number of data is 34. The Voigt bound is the upper limit of the aggregate property, whereas the Reuss bound represents the lower limit and the Hill average is the arithmetic average of the two. V_p is the compressional velocity, V_s is the shear velocity, and V_ϕ is the bulk sound speed; 1 SD errors are in parentheses.

Parameter	Voigt bound	Reuss bound	Hill average
K	247.10	245.70	246.4 (5.0)
μ	184.90	183.50	184.2 (4.0)
V_p	10.96	10.92	10.94
V_s	6.71	6.68	6.69
V_ϕ	7.75	7.73	7.74

Table 3. Comparison of the bulk modulus, K, from this study with the bulk modulus and the assumed pressure derivative of bulk modulus, K', from compression studies for $MgSiO_3$ perovskite; DAC, diamond anvil cell; A, acoustic; errors (1 SD) are in parentheses.

K (GPa)	K'	Maximum pressure	Method	Reference
258 (20)	3 to 5	8.2 GPa	DAC	(*8*)
266 (6)	3.9	127 GPa	DAC	(*9*)
247 (14)	4	9.6 GPa	DAC	(*10*)
246.5 (5)		0.1 MPa	A	*

*This study.

or second order) at high temperatures to a paraelastic phase in which the two orientation states become equivalent. At such a transition, depending on the symmetry of the paraelastic phase, at least one shear modulus commonly goes to zero, and the shear modulus is anomalously low on both sides of the transition as it must smoothly approach zero at the transition temperature.

We were able to transform $MgSiO_3$ perovskite easily from one twin state to the other. Single crystals twin when exposed to laser light levels as low as 5 mW. The speed of this process is related directly with the energy of the laser line. The 6471 Å krypton ion laser radiation did not cause the crystals to twin whereas the 4880 Å Argon laser line induced twinning in a few days at this low power. Acoustic velocities obtained from wavelengths ranging from 4880 Å to 6764 Å did not show any systematic dependence on wavelength. Single-crystal x-ray studies (*13*) have shown that twin-free crystals of perovskite spontaneously twin at temperatures above 100°C. These observations further indicate that perovskite is ferroelastic and that a second-order phase transition at elevated temperatures might occur; such a transition would decrease the shear modulus.

Estimates of the composition of the earth's lower mantle have ranged from pyrolite (silica-poor) to pyroxene (silica-rich) stoichiometries. At lower mantle conditions, these compositions correspond to mineral assemblages of 80% (by volume) perovskite and 20% magnesiowustite to pure perovskite. The compositional models can be tested by a comparison of the elastic properties implied by the composition with those deduced from seismology. Although a large data base is available for the pressure and temperature variation of the elastic properties of magnesiowustite, we have insufficient data to extrapolate the perovskite data from ambient conditions to mantle pressures and temperatures. Instead, we calculated the combinations of $(\partial\mu/\partial T)_P$, $(\partial\mu/\partial P)_S$, $(\partial K/\partial T)_P$, and $(\partial K/\partial P)_S$ for perovskite that are required to match the elastic properties of the preliminary reference earth model, PREM (*14*), at the depth of 1071 km; we did this calculation for both the pyrolite and the pyroxene compositional models with a Fe/(Fe+Mg) ratio of 0.1 and an adiabatic mantle temperature gradient that is 1400°C at zero pressure. Here μ is the shear modulus, K is the bulk modulus, P is pressure, T is temperature, and the subscripts P and S indicate differentiation at constant pressure or entropy. As shown in Fig. 2, whether the lower mantle has a pyrolite or pyroxene composition cannot be resolved on the basis of these new elasticity data. Accurate pressure derivatives of the bulk and shear moduli must be measured in order to determine composition in this manner.

The variation of elastic modulus with depth can be expressed as an adiabatic pressure derivative of that modulus if the temperature gradient is adiabatic. The pressure derivatives of K and μ deduced from the PREM model are illustrated as hatched regions in Fig. 2. The stippled area near the y axis denotes the range of temperature derivatives for various silicate minerals. Thus, the pressure and temperature dependences of the bulk modulus that are required to match the seismic data are similar to what would be expected on the basis of the behavior of other silicates. On the other hand, if the temperature derivative of the shear modulus of perovskite is similar to those of other silicates, it will yield a mantle that is too stiff to match the seismic data. If we adjust the temperature derivative of the shear modulus to match the observed seismic velocities, then the ratio of the temperature derivative of the shear modulus to that of the bulk modulus must be about 3, as opposed to values of less than 1, which are more commonly observed in other silicates.

Recent results from seismic tomography studies (*15*) also indicate that there are anomalously large variations in shear velocity relative to longitudinal velocity in the lower mantle. If the lateral variations are induced by variations in temperature, then

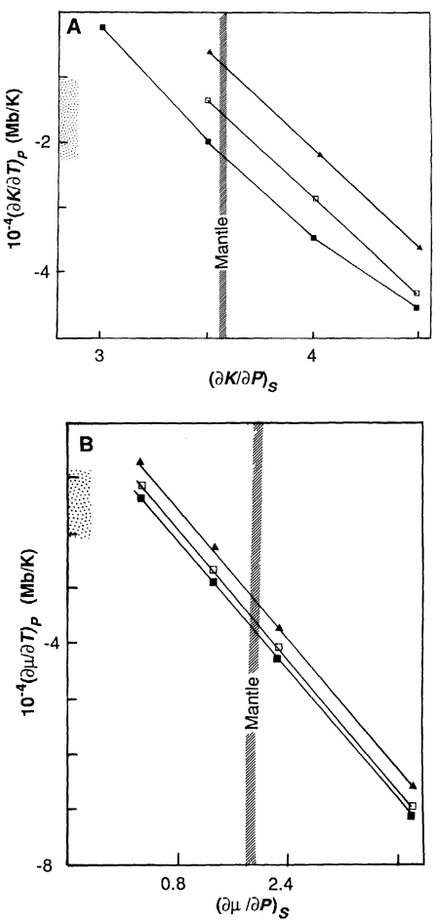

Fig. 2. Trade-off curves for (**A**) $(\partial K/\partial T)_P$ versus $(\partial K/\partial P)_S$ and (**B**) $(\partial\mu/\partial T)_P$ versus $(\partial\mu/\partial P)_S$ for various compositional models of the earth's lower mantle. Filled triangle is for pyrolite; open square is for chondrite; filled square is for pyroxene. The stippled area on the vertical axis denotes the range of temperature derivatives for various silicate phases. The region hatched as "Mantle" illustrates the pressure and temperature dependence of the bulk and shear moduli for these petrological models that are required to match the elastic properties of the PREM model (*14*) at a depth of 1071 km.

again we must conclude that the temperature derivative of the shear modulus must be at least three times that of the bulk modulus.

Whereas the absolute value of the mantle shear modulus can be reconciled by much higher temperatures than we assumed or by a lower mantle Fe/Fe+Mg ratio of at least 0.3, the only conclusion that is also consistent with the seismic tomography is that the lower mantle exhibits an unusually large apparent temperature derivative of the shear modulus as compared to that of the bulk modulus. Recent workers have calculated (*16*) that this ratio cannot exceed unity if perovskite behaves as a normal refractory ceramic with a close-packed oxygen framework. A ferroelastic phase transformation could allow the effective temperature derivative of the shear modulus to be very large, which would account for all of these observations. Such a large negative value will result if the mantle temperature is sufficiently close to that required for a ferroelastic-paraelastic phase transformation in the perovskite phase, so as to induce significant shear mode softening. These transformations are common in perovskite-type compounds and have been predicted theoretically for $MgSiO_3$ (*17*). These phase transformations typically have shallow Clapeyron slopes that could conceivably be parallel to the geothermal gradient. Because other physical properties, including thermal expansion and rheology, will be affected by these transformations, we need to broaden our understanding of this phenomena to determine the physical and chemical properties of the earth's lower mantle.

REFERENCES AND NOTES

1. L. G. Liu, *Nature* **258**, 770 (1976); A. E. Ringwood, *J. Geophys. Res.* **67**, 4005 (1962); E. Ito, E. Takahashi, Y. Matsui, *Earth Planet. Sci. Lett.* **67**, 283 (1984); E. Ito and H. Yamada, in *High Pressure Research in Geophysics*, S. Akimoto and M. H. Manghnani, Eds. (Center for Academic Publishing, Tokyo, 1982), pp. 405–419; T. Yagi, H-K. Mao, P. M. Bell, *Carnegie Inst. Washington Yearb.* **614**, 78 (1979); E. Ito and Y. Matsui, *Earth Planet. Sci. Lett.* **38**, 443 (1978).
2. H. D. Megaw, *Crystal Structures: A Working Approach* (Saunders, Philadelphia, 1973); A. H. Glazer, *Acta Crystallogr. Sec. B* **28**, 3384 (1972); *ibid. Sec. A* **31**, 756 (1975).
3. H. D. Megaw, *Acta Crystallogr.* **5**, 739 (1952); R. Rao and K. J. Rao, *Phase Transitions in Solids* (McGraw-Hill, New York, 1977); J. B. Goodenough and J. M. Longo, in *Landolt-Bornstien New Series, Group III* (Springer-Verlag, Berlin, 1970), vol. 4A, pp. 125–315.
4. Brillouin spectroscopy provides an optical method for measuring acoustic velocities as a function of crystallographic direction in single crystals. Laser light that passes through the sample is Doppler-shifted by the thermally generated acoustic waves. The acoustic velocity is inferred from the measured frequency shift of the scattered light. We are able to determine these properties on single crystals as small as 50 μm, thus allowing these properties to be determined on materials synthesized at high pressure. For additional details of the technique, see D. J. Weidner and H. R. Carleton, *J. Geophys. Res.* **82**, 1334 (1977); D. J. Weidner and M. T. Vaughan, in *High Pressure Science and Technology*, D. Timmerhaus and M. S. Barber, Eds. (Plenum, New York, 1979), vol. 2, pp. 85–90; M. T. Vaughan and J. D. Bass, *Phys. Chem. Minerals* **10**, 62 (1983).
5. E. Ito and D. J. Weidner, *Geophys Res. Lett.* **13**, 464 (1986).
6. D. J. Weidner and E. Ito, *Phys. Earth Planet. Inter.* **40**, 64 (1985); ———, J. D. Bass, A. E. Ringwood, W. Sinclair, *J. Geophys. Res.* **87**, 4740 (1982).
7. R. E. Cohen, *Geophys. Res. Lett.* **14**, 1053 (1987).
8. T. Yagi, H. K. Mao, P. M. Bell, in *Advances in Physical Geochemistry*, S. Saxina, Ed. (Springer-Verlag, New York, 1982), vol. 2, pp. 317–325.
9. E. Knittle and R. Jeanloz, *Science* **235**, 668 (1987).
10. Y. Kudoh, E. Ito, H. Takeda, *Phys. Chem. Minerals* **14**, 350 (1987).
11. K. Aizu, *J. Phys. Soc. Jpn.* **28**, 706 (1970); J. Sapriel, *Phys. Rev. B* **12**, 5128 (1975).
12. S. C. Abrahams, J. L. Bernstein, J. P. Remeika, *Mater. Res. Bull.* **9**, 1613 (1974); ———, R. L. Burns, J. L. Bernstein, *Solid State Commun.* **10**, 379 (1972).
13. R. M. Hazen and N. L. Ross, *Eos* **69**, 473 (1988).
14. A. M. Dziewonski and D. L. Anderson, *Phys. Earth. Planet. Inter.* **25**, 297 (1981).
15. J. H. Woodhouse, A. M. Dziewonski, D. Giardini, X. D. Li, A. Morelli, *Eos* **68**, 356 (1987).
16. O. L. Anderson, T. Goto, D. Isaak, *ibid.*, p. 1488 (1987); E. K. Graham and E. G. Hilbert, *ibid.* **69**, 472 (1988).
17. G. H. Wolf and M. S. T. Bukowinski, in *High Pressure Research in Mineral Physics*, M. H. Manghnani and Y. Syono, Eds. (Terra Scientific, Tokyo, and American Geophysical Union, Washington, DC, 1987), pp. 315–331.

18. This research was supported by NSF grant EAR-85942755.

8 August 1988; accepted 16 December 1988

The Manganese Site of the Photosynthetic Water-Splitting Enzyme

GRAHAM N. GEORGE, ROGER C. PRINCE, STEPHEN P. CRAMER

As the originator of the oxygen in our atmosphere, the photosynthetic water-splitting enzyme of chloroplasts is vital for aerobic life on the earth. It has a manganese cluster at its active site, but it is poorly understood at the molecular level. Polarized synchrotron radiation was used to examine the x-ray absorption of manganese in oriented chloroplasts. The manganese site, in the "resting" (S_1) state, is an asymmetric cluster, which probably contains four manganese atoms, with interatomic separations of 2.7 and 3.3 angstroms; the vector formed by the 3.3-angstrom manganese pair is oriented perpendicular to the membrane plane. Comparisons with model compounds suggest that the cluster contains bridging oxide or hydroxide ligands connecting the manganese atoms, perhaps with carboxylate bridges connecting the 3.3-angstrom manganese pair.

DESPITE EXTENSIVE STUDIES BY X-ray (*1–3*), electron paramagnetic resonance (EPR) (*4*), and optical spectroscopies (*5*), the structure of the manganese (Mn) center of the water-splitting enzyme remains unknown. The enzyme is located in the thylakoid membrane, and during turnover it donates electrons to photosystem II, which are then recovered by the oxidation of H_2O to liberate oxygen (*6*). The enzyme cycles among five different oxidation levels, known as the S states, S_0 through S_4, which are thought to be reflections of different oxidation levels of a multinuclear Mn cluster (*6*). X-ray absorption spectroscopy should be capable of providing a detailed picture of the Mn environment, but, despite much effort (*1–3*), many questions remain.

Experiments were performed at the Stanford Synchrotron Radiation Laboratory on beam lines VI-2 and IV-2 with Si(400) double-crystal monochromators. X-ray absorption was monitored as the x-ray fluorescence excitation spectrum by means of an array of 13 germanium detectors (*7*), with simultaneous measurement of a Mn foil standard [first inflection, 6539.0 eV (*8*)]. Samples were kept dark at 4 K in an Oxford Instruments CF1204 cryostat during data collection. A typical data set (one orientation) represents the average of four to ten scans, each 20 minutes in duration. The oriented spinach chloroplast membranes (*9*) gave no adventitious Mn EPR signals and showed full photoactivity within the reaction centers and their associated redox partners (*9*). Samples were in the dark-adapted S_1 state, and their integrity and orientation were routinely assessed by EPR spectroscopy.

The extended x-ray absorption fine structure (EXAFS) oscillations $\chi(k)$ for individual orientations were fitted by standard methods (*10, 11*). For oriented systems, the EXAFS intensity is approximately proportional to $\cos^2\beta$, where β is the angle between the x-ray electric field vector, **e**, and the absorber-backscatterer vector. Transitions to bound states of predominantly p character have a similar angular dependence, where β is the angle between the axis of the

G. N. George and R. C. Prince, EXXON Research and Engineering Company, Annandale, NJ 08801.
S. P. Cramer, Schlumberger-Doll Research, Ridgefield, CT 06877.